

SEPTEMBER 2018

VOLUME 51

NUMBER 9

[pubs.acs.org/accounts](http://pubs.acs.org/accounts)

# ACCOUNTS

of chemical research



ACS Publications  
Most Trusted. Most Cited. Most Read.

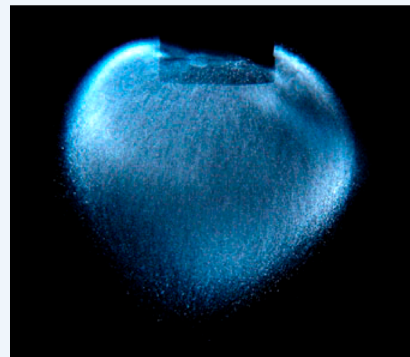
[www.acs.org](http://www.acs.org)

# The Chemical History of a Bubble

Kenneth S. Suslick,<sup>\*†</sup> Nathan C. Eddingsaas,<sup>†</sup> David J. Flannigan,<sup>‡</sup> Stephen D. Hopkins,<sup>§</sup> and Hangxun Xu<sup>⊥</sup>

Department of Chemistry, University of Illinois at Urbana–Champaign, 600 South Mathews Avenue, Urbana, Illinois 61801 United States

**CONSPECTUS:** Acoustic cavitation (the growth, oscillation, and rapid collapse of bubbles in a liquid) occurs in all liquids irradiated with sufficient intensity of sound or ultrasound. The collapse of such bubbles creates local heating and provides a unique source of energy for driving chemical reactions. In addition to sonochemical bond scission and formation, cavitation also induces light emission in many liquids. This phenomenon of sonoluminescence (SL) has captured the imagination of many researchers since it was first observed 85 years ago. SL provides a direct probe of cavitation events and has provided most of our understanding of the conditions created inside collapsing bubbles. Spectroscopic analyses of SL from single acoustically levitated bubbles as well as from clouds of bubbles have revealed molecular, atomic, and ionic line and band emission riding atop an underlying continuum arising from radiative plasma processes. Application of spectrometric methods of pyrometry and plasma diagnostics to these spectra has permitted quantitative measurement of the intracavity conditions: relative peak intensities for temperature measurements, peak shifts and broadening for pressures, and peak asymmetries for plasma electron densities.



The studies discussed herein have revealed that extraordinary conditions are generated inside the collapsing bubbles in ordinary room-temperature liquids: observable temperatures exceeding 15 000 K (i.e., three times the surface temperature of our sun), pressures of well over 1000 bar (more than the pressure at the bottom of the Mariana Trench), and heating and cooling rates in excess of  $10^{12}$  K·s<sup>-1</sup>. Scientists from many disciplines, and even nonscientists, have been and continue to be intrigued by the consequences of dynamic bubbles in liquids. As chemists, we are fascinated by the high energy reactions and processes that occur during acoustic cavitation and by the use of SL as a spectroscopic probe of the events during cavitation. Within the chemical realm of SL and cavitation there are many interesting questions that are now answered but also many that remain to be explored, so we hope that this Account reveals to the reader some of the most fascinating of those curiosities as we explore the chemical history of a bubble.

The high energy species produced inside collapsing bubbles also lead to secondary reactions from the high energy species created within the collapsing bubble diffusing into the bulk liquid and expanding the range of sonochemical reactions observed, especially in redox reactions relevant to nanomaterials synthesis. Bubbles near solid surfaces deform upon collapse, which lessens the internal heating within the bubble, as shown by SL studies, but introduces important mechanical consequences in terms of surface damage and increased surface reactivity. Our understanding of the conditions created during cavitation has informed the applications of ultrasound to a wide range of chemical applications, from nanomaterials to synthetically useful organic reactions to biomedical and pharmaceutical uses. Indeed, we echo Michael Faraday's observation concerning a candle flame, "There is not a law under which any part of this universe is governed which does not come into play and is touched upon in these phenomena." (Faraday, M. *The Chemical History of a Candle*; Harper & Brothers: New York, 1861).

## 1. INTRODUCTION: ACOUSTIC CAVITATION

Imagine a bubble suspended in a liquid, and now send sound through that liquid. The bubble will expand and contract with the expansion and compression waves of the sound. This oscillation, growth, and potential rapid collapse of bubbles is called "acoustic cavitation" and occurs in all liquids irradiated with sufficient intensity of sound or ultrasound. As a cavitating bubble undergoes collapse, one might ideally imagine the compression to be essentially an adiabatic spherical piston. The bubble immediately before the commencement of collapse has some total energy (i.e., from the surface tension and the momentum of the liquid surrounding the bubble). The conversion of that mechanical energy into heat inside the

bubble is the origin of both sonochemistry and sonoluminescence. The temperature rise during collapse depends of course on the bubble radius, but it is not a simple relationship for real vapors (Figure 1).

Chemistry, the making and breaking of bonds between atoms, results from the interaction of energy and matter. The parameters that control that interaction are temperature (i.e., the amount of energy), pressure (the density of interatom collisions), and the time over which the interaction occurs. This three-dimensional space contains all the different kinds of

Received: February 28, 2018

Published: May 17, 2018

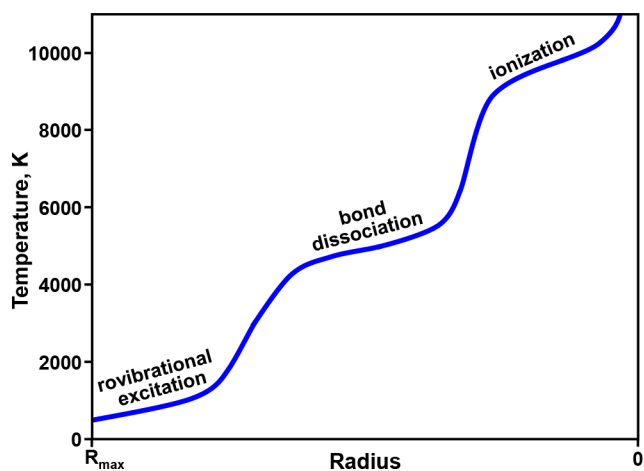


**Figure 1.** Chemical history of an imploding bubble. A simplified conceptual cartoon of the heating of vapor and gas inside a spherical piston undergoing compression as a function of the radius. Rovibrational excitations, endothermic bond dissociations, and eventually ionization limit the rates of temperature rise and the ultimately attainable bubble temperatures during cavitation.

chemistry as islands upon which chemistry occurs (Figure 2). There is much interest in finding new ways of driving chemical reactions along specific potential energy pathways. If one were able to access parameter space that was previously difficult to explore, one would no doubt discover new ways of doing unusual chemistry. Indeed, acoustic cavitation, the formation, growth, and collapse of bubbles in a liquid exposed to ultrasound, opens the door to an interesting part of that parameter space: sonochemical reactions at high pressures, short times, and high temperatures.<sup>1</sup> Our effort to characterize the conditions inside cavitating bubbles is the subject of this Account.

## 2. THE MOVING BUBBLE

The hydrodynamics of cavitation is a well-studied field,<sup>3–5</sup> dating back to Lord Rayleigh's first calculations of enormous pressures during bubble collapse,<sup>6</sup> a study commissioned by the Royal Navy due to their problems with cavitation on propeller

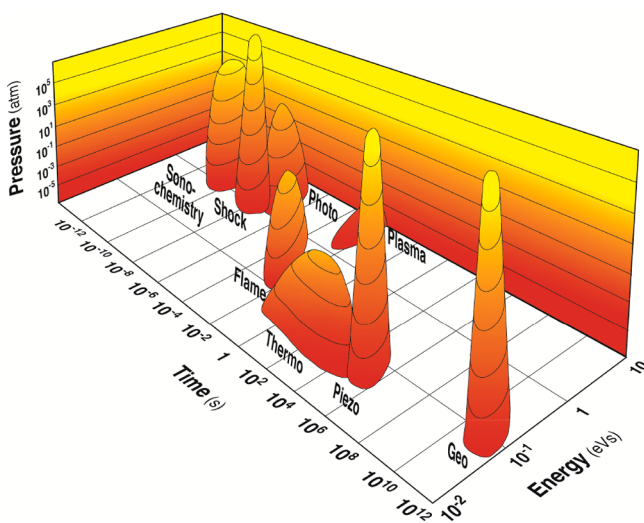


**Figure 2.** Islands of chemistry. Adapted with permission from ref 2. Copyright 2008 Annual Reviews.

surfaces.<sup>7</sup> The Rayleigh–Plesset equation describes individual bubble dynamics with great accuracy, all throughout the cavitation process with the notable exception of the last stages of bubble collapse when the velocity of the bubble wall can exceed the speed of sound. The complexity of the chemical reactions that occur in those final stages dramatically complicates the energy partitioning inside the bubble.<sup>4,5</sup> The need for experimental probes for the conditions inside cavitating bubbles led us to examine sonoluminescence (SL) as a spectroscopic probe.<sup>2</sup> In the sections that follow, we will describe the nature of SL emission and its use to monitor temperatures, pressures, and ionization during bubble collapse.

The dynamics of an isolated single cavitating bubble are shown, both from experiment and from calculation, in Figure 3. These  $r$ – $t$  curves can be experimentally measured by either direct imaging techniques or light scattering.<sup>8,9</sup> Simulations using the RP equation match the experimental data extremely well (Figure 3), at least until the region of maximum compression. For any given acoustic frequency, there is a bubble radius that would be metastable at low acoustic pressures. If we start with such a bubble and expose it to a strong acoustic field, the bubble will grow during the expansion phase of the sound and begin to collapse during the compression phase. Most of that expansion and collapse, however, is relatively slow and consequently isothermal. Not until the very end of the collapse does the bubble surface move so fast as to make the collapse adiabatic. Finally, the bubble undergoes a series of damped oscillations after the initial implosion until coming to rest to await the next rarefaction

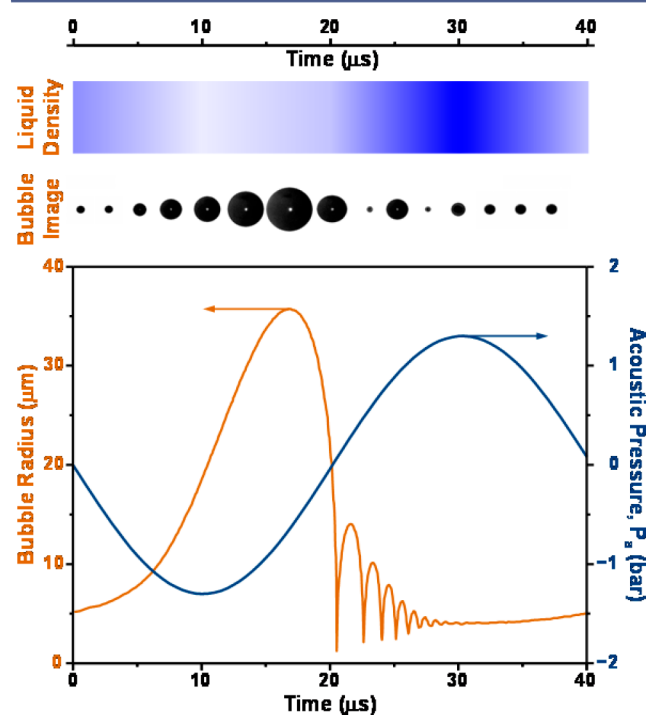


**Figure 3.** Dynamics of an acoustically driven bubble. The time axis applies to all three parts of the figure. The sound field (25 kHz) causes oscillations in the density of the liquid (top). A bubble in the liquid responds by expanding during rarefaction and contracting during compression (stroboscopic single bubble images, middle). The bubble radius vs time curve (bottom) calculated from the Rayleigh–Plesset (RP) equation shows that the radial oscillation is nonlinear even at modest applied acoustic pressures ( $P_a$ ).



phase. To understand how bubble implosion can produce such conditions, the dynamics must be explored. To do this, one typically uses either direct imaging techniques or light scattering.<sup>8,9</sup>

The general case of clouds of bubbles undergoing cavitation is rather more complicated.<sup>2,10–12</sup> First, the formation of bubbles for cavitation is a nucleated process (as it is during boiling, for example) and generally depends on pre-existing gas-filled crevices in solid particulates or on solid surfaces.<sup>10</sup> Once formed, bubbles in a cloud will feel the presence of other nearby bubbles and their compression will no longer be spherical, leading often to formation of microjets in the last stages of collapse. Interfacial instabilities can develop during oscillation, the bubbles can fragment and form “daughter” bubbles that can serve as nucleation sites for future cavitation events. Bubbles can grow through the process of rectified diffusion (a bubble is a pump: its surface area is larger on expansion than during compression, so growth can be faster than shrinking). Bubbles in clouds can coalesce. And, in a cloud, some bubbles may be moving rapidly and others nearly stationary.<sup>13</sup>

The conditions inside collapsing bubbles determine essentially all the chemical consequences of cavitation, and from Rayleigh onward, many have suggested that the intracavity conditions may be extreme. Experimental determination of conditions inside cavitating bubbles were lacking. Due to the highly dynamic nature of cavitation, one cannot simply insert a thermometer into the bubble to measure a temperature. Fortunately, one result of cavitation is the emission of light, sonoluminescence (SL),<sup>14,15</sup> which can occur from either a cloud of bubbles (multibubble sonoluminescence, MBSL)<sup>2,11,16</sup> or a single bubble (single-bubble sonoluminescence, SBSL).<sup>14,15,17–20</sup> In general, there are three classes of devices designed to introduce ultrasound into liquids and thereby generate SL (Figure 4).

### 3. SONOLUMINESCENCE: ATOMS AND MOLECULES INSIDE THE BUBBLE

Since SL was first observed,<sup>21</sup> much work has been devoted to uncovering the origins of this phenomenon, and all early work

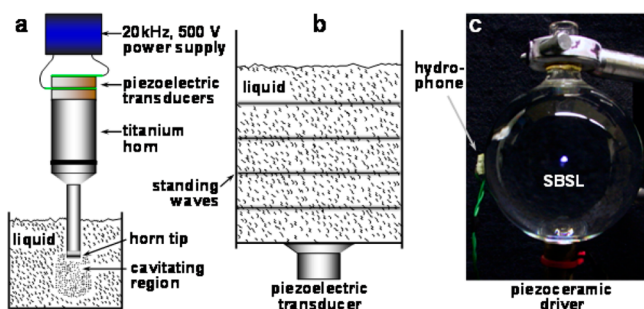


**Figure 4.** Three common apparatus for introducing ultrasound into liquids. (a) An ultrasonic horn is generally the highest intensity source and most versatile for sonochemical studies and multibubble sonoluminescence, used in the 20–50 kHz region. (b) Ultrasonic cleaning bath is a common relatively low intensity apparatus most useful for solid–liquid reactions such as Grignards and lithiations, typically 50 kHz; high frequency, 100 kHz to 1 MHz rigs, have a similar configuration and can be useful for high frequency SL studies. (c) Single bubble cavitation rig, typically 20–100 kHz, are used for physical dynamic and spectroscopic studies of single bubble sonoluminescence.

used clouds of cavitation bubbles. Initial studies of MBSL, which were conducted almost exclusively in water, found the emission spectra to be a convolution of a broad continuum and discrete emission lines of a few partially resolved excited states of OH<sup>•</sup> from H<sub>2</sub>O sonolysis;<sup>22</sup> more recent work argues that the continuum is mainly molecular in origin,<sup>23</sup> but a complete picture is yet to be formulated. The disadvantages of SL from water originate from its very high vapor pressure (even at its freezing point), which dramatically dampens the conditions created during cavitation and consequently results in low emissivity.

Our approach to SL came from our early interest in the sonochemistry of organometallic systems,<sup>16,24–28</sup> and so we began with an exploration of the sonochemistry<sup>24,26</sup> and sonoluminescence<sup>29,30</sup> of nonaqueous liquids with low vapor pressures (Figure 5). MBSL spectra from long-chain hydrocarbons and silicone oils revealed that species well-known in flame spectroscopy, such as C<sub>2</sub> and CH (routinely species produced from burning organics) are formed during cavitation (Figure 5).<sup>31</sup> The dissolution of N<sub>2</sub> (or other nitrogen containing volatiles) or O<sub>2</sub> into the liquid resulted in CN and CO<sub>2</sub> formation and excitation. These emissions were sufficiently intense that they could be vibrationally resolved, and we were able to make the first direct measurements of emission temperatures within the cavitating bubbles.<sup>30</sup> As discussed later, C<sub>2</sub> emission yields emission temperatures of 5100 K.

Our studies of MBSL in nonaqueous liquids included alkali-metal salt solutions,<sup>32</sup> solutions of volatile organometallic compounds,<sup>33–35</sup> room-temperature ionic liquids (RTILs),<sup>36,37</sup>

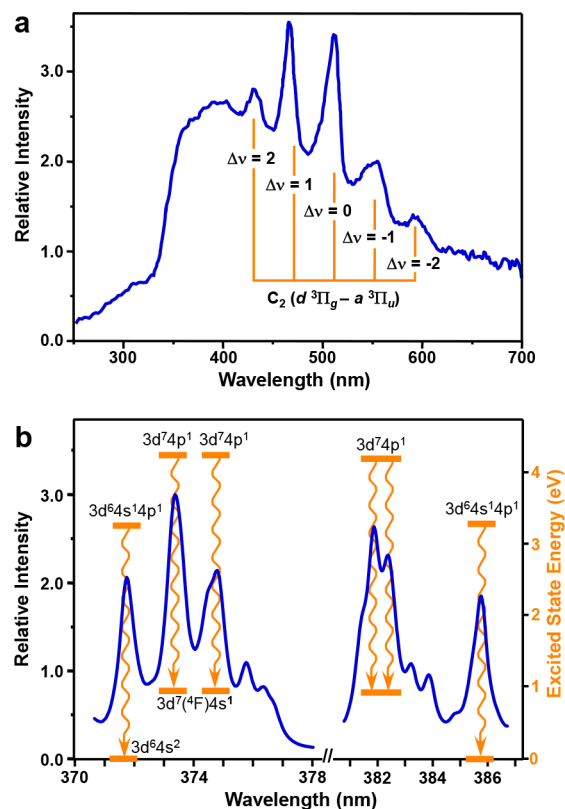


**Figure 5.** Examples of MBSL spectra: (a) C<sub>2</sub> emission from dodecane; (b) Fe atom emission from Fe(CO)<sub>5</sub> in silicone oil. Adapted with permission from ref 2. Copyright 2008 Annual Reviews.

and nearly water-free acids<sup>13,34,38–40</sup> (e.g., concentrated sulfuric and phosphoric acids). MBSL spectra from these liquids were found to depend on the components of the solution from which they were generated; as Tom Lehrer once nearly said, life is like a bubble: what you get out of it depends on what you put into it.<sup>41</sup> MBSL from both volatile and involatile emitters was observed. For example, the spectral features from alkali-metal salt solutions are lines from the neutral metal atoms coming from nonvolatile ionic salts,<sup>32,33</sup> and in various RTILs,<sup>36</sup> regardless of the negligible vapor pressures of the ionic liquids, emission lines from excited-state radicals (e.g., C<sub>2</sub>, CN, and CH generated from sonolysis of the involatile liquid) were still observed.

The origin of the unexpected emission from nonvolatile species during MBSL remained a central question in the mechanism of acoustic cavitation because it implied heating of some liquid during the cavitation process. Two general models for the sonochemistry and sonoluminescence from nonvolatile compounds dissolved in solution have been proposed,<sup>5,28,34</sup> heated shell vs injected droplet models, as shown in Figure 6, but no previous work had been able to differentiate between them.

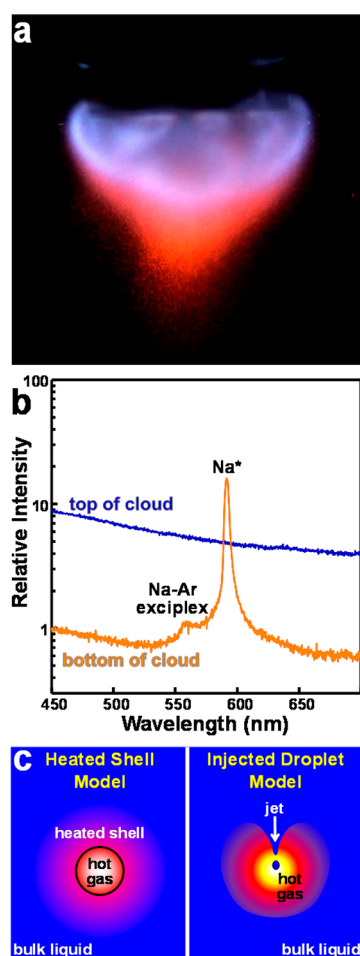


**Figure 6.** (a) Photograph of MBSL from an ultrasonic horn in sulfuric acid with dissolved Na<sub>2</sub>SO<sub>4</sub>. (b) MBSL spectra taken at the top and the bottom of the cavitating bubble cloud. (c) Two-site models of sonochemical activity. Adapted with permission from ref 13. Copyright 2009 American Chemical Society.

For this reason, we examined sulfuric acid solutions (whose sonoluminescence intensity is hundreds to thousands of times more intense than aqueous solutions<sup>42</sup> and therefore easily studied in spectroscopic detail) into which sodium sulfate had been dissolved.<sup>13</sup> We discovered that MBSL from sulfuric acid solutions of Na<sup>+</sup> ions permitted us to observe two distinct sonoluminescing bubble populations (Figure 6), which provided the first experimental evidence for the injected droplet model over the heated-shell model for cavitation.<sup>13</sup> Intense orange-yellow emission (from involatile sodium atom excited states) was observed some distance from the ultrasonic horn whereas only blue-white emission was observed near the horn. If the heated-shell model were correct, then a spatial separation of different sonoluminescence emitters *ought not to occur*. For the heated-shell model, SL from nonvolatile species should always be present whenever conditions are sufficient to give rise to SL inside the bubble. If the nanodroplet model applied, then only in bubbles that collapsed asymmetrically would jetting occur creating nanodroplets that enter the hot interior of the bubble, where complex redox processes analogous to those in flames generate the Na atom excited states.

In cavitating bubble clouds, there are two distinct populations of cavitation events: (1) bubbles near the vibrating horn that are relatively stationary (probably due to interbubble Bjerknes forces), whose collapse is highly symmetric, which produces a hotter core and only continuum emission, and (2) rapidly moving bubbles in streaming liquid flow outside of the dense clouds, whose collapse is much less symmetric and from which emission from nonvolatile species becomes possible through the mechanism of nanodroplet injection<sup>13</sup> (Figure 6); direct observations of these bubble populations by high speed video<sup>43</sup> confirms our earlier studies. Distortions during bubble collapse are also possible during single bubble cavitation again producing emission from nonvolatile species.<sup>44</sup>

#### 4. EXOTIC BUBBLES: SINGLE BUBBLE SONOLUMINESCENCE IN IONIC LIQUIDS

The vast majority of SBSL studies have been conducted in water,<sup>18–20</sup> due in part to the chemophobicity of most physicists and in part to the spatial stability of single bubbles cavitating in water (which is a function of dissolved gas solubility and viscosity). In the early studies of SBSL in water, it was observed that an air-filled bubble was not initially spatially stable, but that after some time the bubble would become so. Lohse suggested<sup>45</sup> that the N<sub>2</sub> and O<sub>2</sub> could react inside the cavitating bubble and the resulting NO<sub>x</sub> would dissolve out into the liquid, thus leaving only Ar behind inside the bubble at roughly 0.01 bar, which coincidentally is in the stable regime for single bubble cavitation;<sup>46</sup> we were able to confirm this hypothesis by the quantification of the NO<sub>x</sub> produced.<sup>47</sup>

Water, however, is actually a poor choice for SL studies given its high vapor pressure: (1) polyatomic content inside the bubble substantially diminishes the polytropic ratio ( $C_p/C_v$ ) that determines the rise in temperature upon compression and (2) the amount of energy needed to dissociate the water vapor inside a single bubble is roughly equal to the total potential energy of the bubble at maximum size before its collapse.<sup>47,48</sup> In addition, SBSL spectra from water give rather limited information since the spectra typically consist of only a smooth continuum stretching from the near-IR to the near-UV.<sup>49</sup> These featureless spectra, in combination with picosecond flash widths<sup>50</sup> and detailed simulations of the bubble dynamics,<sup>4,51,52</sup>

indicate the existence of extreme conditions. Analysis of the featureless SBSL spectra, however, provides little definitive information about the intracavity conditions or light emitting mechanisms, due to the numerous processes that can produce continuous emission (e.g., blackbody, bremsstrahlung, ion–electron recombination, pressure-broadened discrete electronic transitions, etc.), and quantitative descriptions from continuum spectra of unknown origins are inherently model-dependent.<sup>53,54</sup>

We therefore chose to explore a variety of nonaqueous liquids for SBSL. There are two criteria of importance here: first, the liquid must have low volatility to avoid the  $C_p/C_v$  problem, and second, volatile products from the inevitable sonolysis of even low volatility liquids must have high solubility in the liquid to avoid the buildup of volatile species inside a single bubble over millions of cycles of growth and collapse. Both criteria are important: dodecane or silicone oils have low vapor pressures but do not fit the second criterion, and SBSL is rapidly quenched as the bubble self-poisons. In contrast, SBSL from polar aprotic organic liquids, e.g., formamide, can be several times brighter than that from water.<sup>55</sup> More strikingly, we discovered that SL generated from mineral acids (e.g., sulfuric or phosphoric acids), which satisfy both of these criteria, proved to give much higher emission intensities during SBSL (often by >1000-fold).<sup>42</sup>

Perhaps the most important discovery from our studies of SL from  $H_2SO_4$  was the observation of extensive molecular, atomic, and ion emission in the spectra. The spectral profiles are dominated by molecular emission bands from sonolysis products of  $H_2SO_4$  and by emission from gas dissolved in solution. For example, strong atomic Ar lines emerge in the SBSL spectrum from  $H_2SO_4$  containing Ar gas dependent upon the acoustic pressure driving the bubble (Figure 7); as discussed later, this permitted the first experimental measurements of temperature during SBSL.<sup>42</sup> Both SBSL and MBSL from concentrated  $H_2SO_4$  show emission bands from SO as well as intense emission lines from Ar or other dissolved noble gases.<sup>38</sup> The observation of emission from noble gas atoms was the first line emission ever observed during SBSL and permitted, as discussed next, a direct experimental measure-

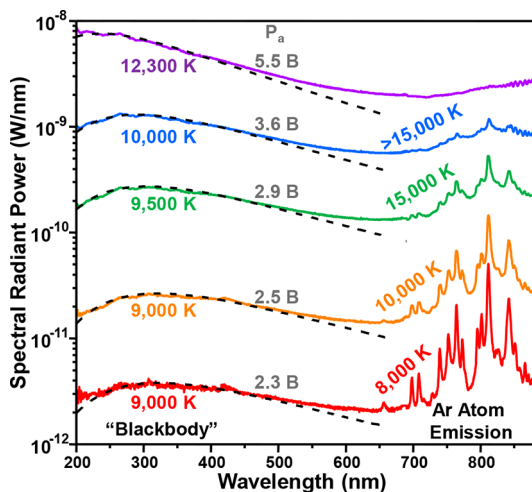


**Figure 7.** SBSL from 85 wt %  $H_2SO_4$ (aq) with 5% Ar. The acoustic pressure at which the bubble was driven is shown below the corresponding spectrum. Adapted with permission from ref 42. Copyright 2005 Nature Publishing Group.

ment of emission temperatures. The populated states of the noble gas atoms are high in energy (e.g., 13 eV for Ar and 20 eV for Ne) indicating that the intracavity conditions generated during SL in  $H_2SO_4$  may be extreme, even by most cavitation standards, a matter that we will return to in our discussion of the plasma core inside some cavitating bubbles.

The improved intensity of SL from sulfuric and phosphoric acid also permitted for the first time characterization of the morphology of the active bubble cloud.<sup>13,38,40</sup> The shape of the cloud of cavitating bubbles that produce SL depends on the acoustic intensity from the ultrasonic horn, as shown in Figure 8. As was mentioned in the earlier discussion of emission from sodium excited states, the MBSL spectral profiles depend upon location in these clouds, which implies different conditions exist for individual bubbles within cavitating clouds: some bubbles are stationary, some move rapidly, some collapse more symmetrically, and some collapse quite asymmetrically. The

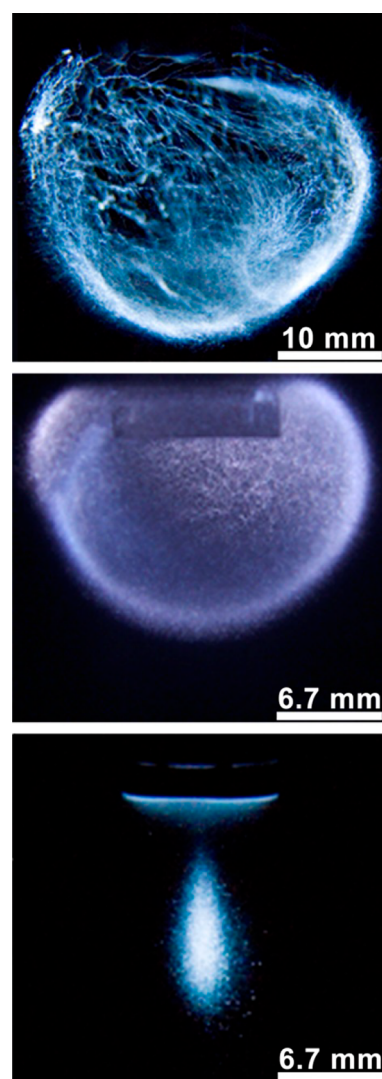


**Figure 8.** MBSL comes from complex clouds of bubbles that depend upon the acoustic intensity radiated by an ultrasonic horn. Photographs (10 s exposures) of MBSL from  $H_2SO_4$  saturated with Ar: (top to bottom) filamentous, bulbous, and cone shaped emission at 14, 22, and 30  $W/cm^2$ , respectively. The tip of the ultrasonic horn is at the top. Adapted with permission from ref 38. Copyright 2007 American Chemical Society.



dynamics of bubbles inside these clouds are complex, and the cooperative motion of bubbles have both spatial and temporal correlations that are not yet fully understood.<sup>12</sup>

## 5. INSIDE A COLLAPSING BUBBLE: CONDITIONS DURING CAVITATION

### 5.1. Temperature inside the Bubble

Emission lines observed in the SL spectra provide unambiguous information about the species generated during cavitation. With well-defined lines, one may use relative peak intensities to determine temperatures, peak shifts for pressures, and peak asymmetry for plasma electron densities. In general, given known transition probabilities and energies of the excited states, spectra can be easily calculated for most atomic and many diatomic emitters at any given temperature and then matched for best fit to experimental observations.<sup>56</sup> This is the same technique used to quantify the conditions of high-temperature sources (e.g., flames) and remote locations (e.g., stellar surfaces).

Sonication of solutions of volatile metal carbonyl complexes, for example, results in emission from the neutral metal atoms (Figure 5).<sup>33</sup> The relative intensities of the emission lines can be used to determine effective MBSL temperatures. For example, from a solution of  $\text{Cr}(\text{CO})_6$  in silicone oil saturated with Ar, we determined an emission temperature of  $4700 \pm 300$  K from the relative intensities of Cr atom emission lines (Figure 9).<sup>35</sup> Under the same MBSL conditions, the emission temperatures from  $\text{C}_2$ , Mo, and Fe were, respectively,  $4900 \pm 300$ ,  $4800 \pm 300$ , and  $5100 \pm 350$  K, giving some assurance of local thermodynamic equilibrium under this set of conditions.<sup>30</sup>

Polyatomic content inside cavitating bubbles has a substantial effect on the compressional heating. Sulfuric and phosphoric acids (with very low vapor pressures) gave MBSL emission temperatures as high as 8000 and 9500 K, respectively.<sup>38,40</sup> Silicone oil, which produces some volatile hydrocarbons during sonolysis, has an effective vapor pressure somewhat greater than the acids. And as expected for water's greater vapor pressure, similar temperature measurements of cavitation in

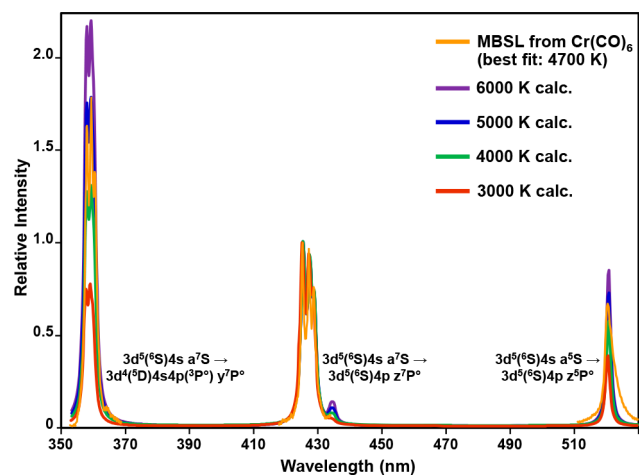


**Figure 9.** Cr atom emission lines in the MBSL spectrum from 2.5 mM  $\text{Cr}(\text{CO})_6$  in silicone oil saturated with Ar. The Cr emission is compared to synthetic spectra at various temperatures. The spectrum is best fit by emission at 4700 K. Adapted with permission from ref 2. Copyright 2008 Annual Reviews.

water (doped with trace benzene to provide  $\text{C}_2$  emission) gave somewhat lower temperatures (4300 K).<sup>57</sup>

Since the first reports of the properties of SBSL, many have speculated that the intracavity conditions may be even more extraordinary than those generated during MBSL: the symmetry of bubble collapse should be maintained more rigorously in SBSL leading to greater compression. Observation of emission lines in the SBSL spectra from  $\text{H}_2\text{SO}_4$  (Figure 7) provided a means for quantitative analysis in the same manner as was employed for MBSL. As shown in Figures 7 and 10, SBSL emission temperatures are dependent on the driving acoustic pressure and can exceed 15000 K as measured from

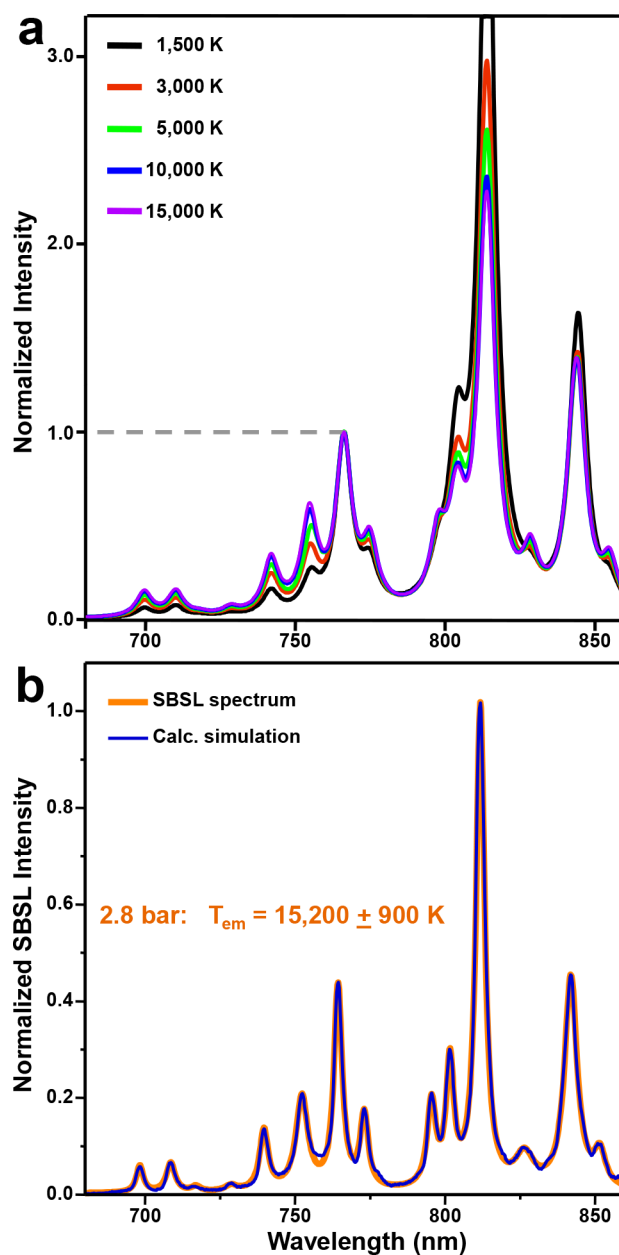


**Figure 10.** Ar atom emission temperatures during SBSL. (a) Calculated synthetic spectra for Ar as a function of temperature, normalized to the peak intensity at 763 nm. (b) SBSL Ar atom line emission at  $P_a = 2.8$  is compared to its best fit synthetic spectrum at 15200 K. Adapted with permission from ref 42. Copyright 2005 Nature Publishing Group.

the relative intensities of Ar atom emission lines.<sup>42</sup> Distortion of single bubble collapse by introduction of a glass surface near the bubble has the expected effect of systematically lowering the emission temperature as the perturbation is increased.<sup>58</sup>

### 5.2. Pressure inside the Bubble

The simplest estimates of pressures assume adiabatic compression and ideal gas behavior. Given an emission temperature, within those assumptions, MBSL predicts compression ratios of 4.0 (for 5000 K final temperature), which then predicts a final pressure of  $\sim 1000$  bar (i.e., 100 MPa).

Measurement of intracavity pressures generated during MBSL can make use of the peak shifts and peak widths of emission lines from electronically excited atoms.<sup>59</sup> By comparing the observed shift of the MBSL Cr\* lines (Figure 8, vs low pressure Cr emission) to the ballistic compressor data and extrapolating to temperatures observed during cavitation (4700 K), pressures of  $300 \pm 30$  bar were determined. Because the ballistic compressor data showed that the degree of Cr\* line red shift decreased with increasing temperature, the pressure of 300 bar was taken as a lower limit.

Analysis of the densities and pressures generated during SBSL must separate broadening due to pressure from that due to Stark effects (from ionization) and instrument response.<sup>60</sup> For Ar emission, SBSL temperature of 10000 K, the observed line broadening (Figure 11) produces a calculated density of  $10^{21}$  Ar atoms·cm<sup>-3</sup> for modest acoustic pressures. Application of the van der Waals equation of state to the determined Ar density and temperature then gives SBSL pressure of 1400 bar. This density and pressure match very well with those determined from the measured bubble dynamics and the simple adiabatic compression model. At elevated  $P_a$ , where the Ar lines become broadened to the point of being indistinguishable from the underlying continuum, the bubble dynamics method estimates increased pressures of  $>3700$  bar.<sup>60</sup>

### 5.3. Temporal Measurements

Using time-correlated single photon counting, researchers have found that the pulse width of the light flash can last anywhere from  $\sim 60$  to 350 ps for a single bubble in water.<sup>50</sup> Furthermore, by using picosecond resolved light scattering and simulation,<sup>51,62</sup> researchers have found that the single bubble radius contracts by more than a factor of 100 within a few microseconds during implosion, reaching velocities of Mach 4 and having accelerations<sup>9</sup> at the turnaround point as high as  $10^{11}$ g. In sulfuric and phosphoric acid (which are considerably more viscous), SBSL is slower with emission times of several nanoseconds, but with several thousand-fold greater light emission than water.<sup>42</sup>

Emission time measurements of MBSL are much more difficult compared to SBSL, where one knows both the position and the time of the next cavitation event; nonetheless, MBSL emission times have also been measured and found to be on the order of a few nanoseconds.<sup>63</sup> This means that the heating and cooling rates associated with SL routinely exceed  $10^{12}$  K·s<sup>-1</sup>. In the case of SBSL, where the emission can be shorter than 100 ps,<sup>50</sup> rates on the order of  $10^{14}$  K·s<sup>-1</sup> may be reached.

## 6. OPAQUE PLASMA CORE: WHAT LURKS WITHIN THE BUBBLE?

It had long been predicted that single bubble cavitation might create conditions sufficient to create plasma inside the collapsing bubble,<sup>51,52,64</sup> but direct experimental evidence

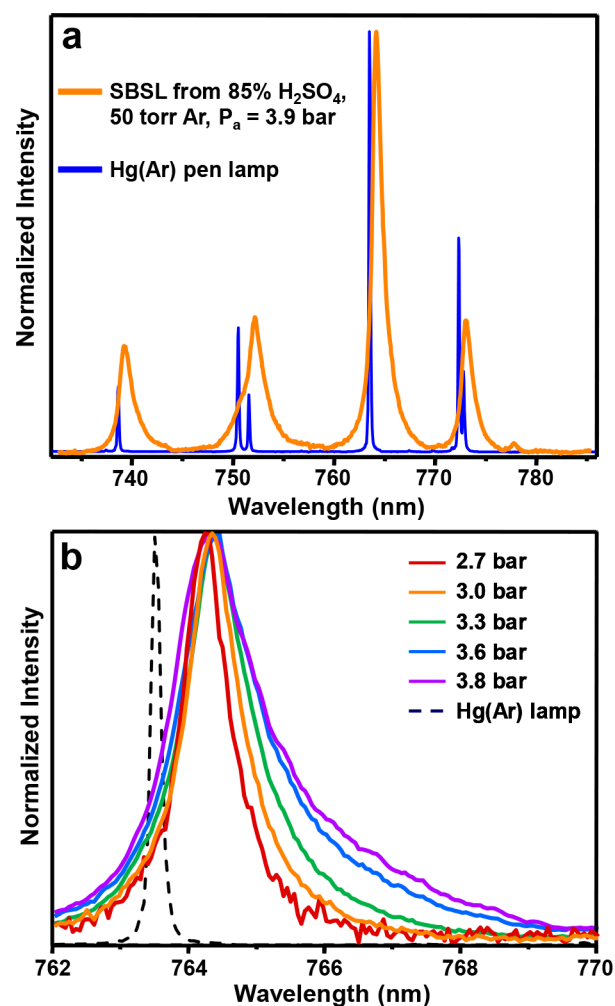


**Figure 11.** Line shifts, broadening, and asymmetry from Ar atom emission during SBSL. (a) SBSL line shifts compared to low pressure Ar atom emission. (b) Line broadening and increasing asymmetry with increasing  $P_a$ . Adapted with permission from ref 61. Copyright 2010 Nature Publishing Group.

took some time to develop. Observation of line emission during both SBSL and MBSL in mineral acids provided valuable information about the intracavity conditions and chemical processes,<sup>38,65</sup> but the presence of noble gas atom emission (Figures 7, 10, and 12) also revealed a paradox: the states involved in the observed electronic transitions for Ne, Ar, Kr, and Xe are very high in energy relative to the ground states of the neutral atoms. The Ar neutral atom transitions (Figure 10), for example, arise from the 4s–4p manifold at  $\sim 11.6$  eV and  $\sim 13.3$  above the ground state ( $3p^6$ ), which cannot be thermally populated if the temperature of the entire bubble were only 15000 K (i.e., 1.3 eV).<sup>42</sup> So the apparent paradox is that we have local thermodynamic equilibrium (LTE) in excited states that cannot be reached thermally. Indeed, upon closer examination of the SBSL from sulfuric acid, we made direct observation of plasma lines in the first ion emission lines ever found for any SL.<sup>65</sup> One observes emission from Ar<sup>+</sup>, Kr<sup>+</sup>, and Xe<sup>+</sup> coming from excited states that are 37, 33, and 27 eV above the neutral ground states (Figure 12). Here too, thermal ionization is simply implausible at the measured emission temperatures. The asymmetry of the emission lines (Figure 10) also permit the estimation of the electron plasma density, with



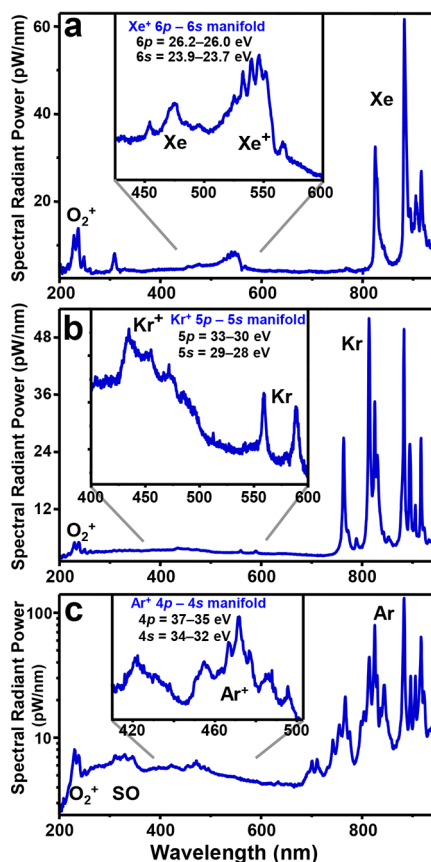


**Figure 12.** Noble gas and ion emission lines during SBSL. Adapted with permission from ref 65. Copyright 2005 American Physical Society.

$N_e$  found to exceed  $10^{21} \text{ cm}^{-3}$ , comparable to the densities produced in laser-driven fusion experiments.<sup>61</sup>

Confirmation of the presence of a plasma in the collapsing bubble comes from the observation of  $\text{O}_2^+$  emission<sup>42</sup> (Figure 12), the first ion emission ever observed during SL. The bond energies of  $\text{O}_2$  and  $\text{O}_2^+$  are 5.1 and 6.5 eV, respectively, while the ionization energy of  $\text{O}_2$  is much higher (12.1 eV). The formation and excitation of  $\text{O}_2^+$  therefore cannot occur thermally: rather,  $\text{O}_2^+$  is produced by high energy electron impact, in this case from the hot, opaque plasma core of the SL bubble.

So the measured emission temperatures from both SBSL and MBSL must only hint at what occurs in the very core of a collapsing bubble and suggest the presence (at least in some liquids under some conditions) of a transient, hidden, optically opaque core of higher energy still.<sup>42,61,65,66</sup> The excitation mechanism leading to population of these high energy states is impact from plasma electrons; observation of noble gas ion emission during SBSL from  $\text{H}_2\text{SO}_4$  provides strong support for this proposition. These observations provided the first strong experimental evidence for plasma formation during acoustic cavitation.

The presence of this opaque plasma core during SL has been confirmed recently by time-resolved studies with comparable  $N_e$  estimates, and the lowering of ionization potentials by ion shielding in the dense plasma demonstrated.<sup>67–70</sup> Under these conditions, the SL observed is not from the very core of the cavitating bubble, but rather comes from the outer border of the plasma core, analogous to the photosphere of a star.

## 7. CONCLUSIONS AND OUTLOOK

The chemical consequence of cavitation has emerged as the general field of sonochemistry over the past 40 years. The chemical history of a bubble as it collapses has been explored using sonoluminescence, a spectroscopic probe of the conditions created during implosion. SL has been able to produce quantitative measurements of the temperatures, pressures, and lifetimes inside collapsing bubbles and under some conditions even the extent of ionization in plasmas. Secondary reactions from the high energy species created within the collapsing bubble diffuse into the bulk liquid and expand the range of sonochemical reactions observed, especially in redox reactions relevant to nanomaterials synthesis.<sup>71,72</sup> Bubbles near solid surfaces deform upon collapse, which lessens the internal heating within the bubble, as shown by SL studies,<sup>58</sup> but introduces important mechanical consequences in terms of surface damage and increased surface reactivity.<sup>16,73,74</sup> Our understanding of the conditions created during cavitation has informed the applications of ultrasound to a wide range of chemistry, from nanomaterials to important synthetic organic and organometallic reactions to biomedical, drug delivery, and pharmaceutical uses.<sup>16,71–77</sup>

## AUTHOR INFORMATION

### Corresponding Author

\*E-mail: ksuslick@illinois.edu.

### ORCID

Kenneth S. Suslick: 0000-0001-5422-0701

David J. Flannigan: 0000-0002-1829-1868

Hangxun Xu: 0000-0003-1645-9003

### Present Addresses

<sup>†</sup>Rochester Institute of Technology, Rochester, NY 14623, United States.

<sup>‡</sup>University of Minnesota, Minneapolis, MN 55455, United States.

<sup>§</sup>Intel Corporation, Santa Clara, CA 95054, United States.

<sup>‡</sup>University of Science and Technology of China, Hefei, 230000 Anhui, China.

### Notes

The authors declare no competing financial interest.

### Biographies

**Kenneth S. Suslick** is the *Marvin T. Schmidt* Research Professor of Chemistry at the University of Illinois at Urbana–Champaign. Professor Suslick received his B.S. from Caltech in 1974 and his Ph.D. from Stanford in 1978 and came to the University of Illinois immediately thereafter. Among his awards are the Centenary Prize and the Sir George Stokes Medal of the RSC, the MRS Medal, the ACS Nobel Laureate Signature and Cope Scholar Awards, the Helmholtz-Rayleigh Silver Medal of the ASA, and the Chemical Pioneer Award of the AIC. He is a Fellow of the National Academy of Inventors.

**Nathan C. Eddingsaas** is an Assistant Professor at the Rochester Institute of Technology. He received his undergraduate degrees in chemistry and aquatic toxicology from the University of Wisconsin—Stevens Point in 2003 and his Ph.D. in chemistry from UIUC in 2008 where he studied mechanoluminescence and sonoluminescence from acoustic cavitation. He was a postdoctoral researcher with Prof. P. O. Wennberg at Caltech.

**Stephen D. Hopkins** is currently a senior engineer at Intel Corporation. He received his B.S. in chemistry from Washington

and Lee University in 2000 and his Ph.D. in chemistry in 2006 from UIUC where he studied the energetics of acoustic cavitation generated in high-Q resonators.

**Hangxun Xu** is a professor at the University of Science and Technology of China. He received his B.S. degree in 2006 from USTC and his Ph.D. in Materials Chemistry in 2011 from UIUC. Thereafter, he was a Postdoctoral Research Associate with Prof. John Rogers in MatSE at UIUC.

**David J. Flannigan** is an Associate Professor in Chemical Engineering and Materials Science at the University of Minnesota. He received his B.S. from U. Minn. in 2001 and Ph.D. from UIUC in 2006 and then was a postdoctoral associate with Prof. A. H. Zewail at Caltech.

## ACKNOWLEDGMENTS

We thank all the Suslick Group members, past and present, that have contributed over the past 40 years to our sonochemical and sonoluminescence studies. This work was supported by the NSF and DARPA.

## REFERENCES

- (1) Suslick, K. S. Sonochemistry. *Science* **1990**, *247*, 1439–1445.
- (2) Suslick, K. S.; Flannigan, D. J. Inside a Collapsing Bubble: Sonoluminescence and the Conditions During Cavitation. *Annu. Rev. Phys. Chem.* **2008**, *59*, 659–683.
- (3) Leighton, T. G. *The Acoustic Bubble*; Academic Press: San Diego, CA, 1994.
- (4) Yasui, K. *Acoustic Cavitation and Bubble Dynamics*; Springer: Cham, 2018.
- (5) Prosperetti, A. Vapor Bubbles. In *Annual Review of Fluid Mechanics*; Davis, S. H., Moin, P., Eds.; Annual Reviews: 2017; Vol. 49, pp 221–248.
- (6) Rayleigh, L. On the Pressure Developed in a Liquid During the Collapse of a Spherical Cavity. *Philos. Mag.* **1917**, *34*, 94–98.
- (7) Thornycroft, J.; Barnaby, S. W. Torpedo-Boat Destroyers. *Proc. Inst. Civil Eng.* **1895**, *122*, 51–69.
- (8) Tian, Y.; Ketterling, J. A.; Apfel, R. E. Direct Observation of Microbubble Oscillations. *J. Acoust. Soc. Am.* **1996**, *100*, 3976–3978.
- (9) Weninger, K. R.; Evans, P. G.; Putterman, S. J. Time Correlated Single Photon Mie Scattering from a Sonoluminescing Bubble. *Phys. Rev. E: Stat. Phys., Plasmas, Fluids, Relat. Interdiscip. Top.* **2000**, *61*, R1020–R1023.
- (10) Brennen, C. E. *Cavitation and Bubble Dynamics*; Cambridge University Press: Cambridge, 2014.
- (11) Suslick, K. S.; Didenko, Y.; Fang, M. M.; Hyeon, T.; Kolbeck, K. J.; McNamara, W. B.; Mdeleeni, M. M.; Wong, M. Acoustic Cavitation and Its Chemical Consequences. *Philos. Trans. R. Soc., A* **1999**, *357*, 335–353.
- (12) Yasui, K.; Iida, Y.; Tuziuti, T.; Kozuka, T.; Towata, A. Strongly Interacting Bubbles under an Ultrasonic Horn. *Phys. Rev. E* **2008**, *77*, 016609.
- (13) Xu, H. X.; Eddingsaas, N. C.; Suslick, K. S. Spatial Separation of Cavitating Bubble Populations: The Nanodroplet Injection Model. *J. Am. Chem. Soc.* **2009**, *131*, 6060–6061.
- (14) Suslick, K. S.; Matula, T. J. Acoustic Cavitation, Sonochemistry, and Sonoluminescence. In *Wiley Encyclopedia of Electrical and Electronics Engineering*; Webster, J. G., Ed.; Wiley-Interscience: New York, 1999; Vol. 22, pp 646–657.
- (15) Walton, A. J.; Reynolds, G. T. Sonoluminescence. *Adv. Phys.* **1984**, *33*, 595–660.
- (16) Suslick, K. S. Synthetic Applications of Ultrasound. *Mod. Synth. Methods* **1986**, *4*, 1–60.
- (17) Gaitan, D. F.; Crum, L. A.; Church, C. C.; Roy, R. A. Sonoluminescence and Bubble Dynamics for a Single, Stable, Cavitation Bubble. *J. Acoust. Soc. Am.* **1992**, *91*, 3166–3183.
- (18) Putterman, S. J.; Weninger, K. R. Sonoluminescence: How Bubbles Turn Sound into Light. *Annu. Rev. Fluid Mech.* **2000**, *32*, 445–476.
- (19) Brenner, M. P.; Hilgenfeldt, S.; Lohse, D. Single-Bubble Sonoluminescence. *Rev. Mod. Phys.* **2002**, *74*, 425–484.
- (20) Crum, L. A. Resource Paper: Sonoluminescence. *J. Acoust. Soc. Am.* **2015**, *138*, 2181–2205.
- (21) Frenzel, H.; Schultes, H. Lumineszenz Im Ultraschallbeschickten Wasser. *Z. Phys. Chem.* **1934**, *B27*, 421–424.
- (22) Taylor, K. J.; Jarman, P. D. Spectra of Sonoluminescence. *Aust. J. Phys.* **1970**, *23*, 319–334.
- (23) McNamara, W. B., III; Didenko, Y. T.; Suslick, K. S. The Nature of the Continuum in Multibubble Sonoluminescence. *J. Am. Chem. Soc.* **2000**, *122*, 8563–8564.
- (24) Suslick, K. S.; Gawienowski, J. J.; Schubert, P. F.; Wang, H. H. Alkane Sonochemistry. *J. Phys. Chem.* **1983**, *87*, 2299–2301.
- (25) Suslick, K. S.; Goodale, J. W.; Schubert, P. F.; Wang, H. H. Sonochemistry and Sonocatalysis of Metal Carbonyls. *J. Am. Chem. Soc.* **1983**, *105*, 5781–5785.
- (26) Suslick, K. S.; Gawienowski, J. J.; Schubert, P. F.; Wang, H. H. Sonochemistry in Non-Aqueous Liquids. *Ultrasonics* **1984**, *22*, 33–36.
- (27) Suslick, K. S.; Schubert, P. F.; Goodale, J. W. Sonochemistry and Sonocatalysis of Iron Carbonyls. *J. Am. Chem. Soc.* **1981**, *103*, 7342–7344.
- (28) Suslick, K. S.; Hammerton, K. A.; Cline, R. E., Jr The Sonochemical Hot Spot. *J. Am. Chem. Soc.* **1986**, *108*, 5641–5642.
- (29) Suslick, K. S.; Flint, E. B. Sonoluminescence from Nonaqueous Liquids. *Nature* **1987**, *330*, 553–555.
- (30) Flint, E. B.; Suslick, K. S. The Temperature of Cavitation. *Science* **1991**, *253*, 1397–1399.
- (31) Gaydon, A. G. *The Spectroscopy of Flames*, 2nd ed.; John Wiley & Sons, Inc.: New York, 1974.
- (32) Flint, E. B.; Suslick, K. S. Sonoluminescence from Alkali-Metal Salt-Solutions. *J. Phys. Chem.* **1991**, *95*, 1484–1488.
- (33) Suslick, K. S.; Flint, E. B.; Grinstaff, M. W.; Kemper, K. A. Sonoluminescence from Metal-Carbonyls. *J. Phys. Chem.* **1993**, *97*, 3098–3099.
- (34) Didenko, Y. T.; McNamara, W. B., III; Suslick, K. S. Effect of Noble Gases on Sonoluminescence Temperatures During Multibubble Cavitation. *Phys. Rev. Lett.* **2000**, *84*, 777–780.
- (35) McNamara, W. B.; Didenko, Y. T.; Suslick, K. S. Sonoluminescence Temperatures During Multi-Bubble Cavitation. *Nature* **1999**, *401*, 772–775.
- (36) Oxley, J. D.; Prozorov, T.; Suslick, K. S. Sonochemistry and Sonoluminescence of Room-Temperature Ionic Liquids. *J. Am. Chem. Soc.* **2003**, *125*, 11138–11139.
- (37) Flannigan, D. J.; Hopkins, S. D.; Suslick, K. S. Sonochemistry and Sonoluminescence in Ionic Liquids, Molten Salts, and Concentrated Electrolyte Solutions. *J. Organomet. Chem.* **2005**, *690*, 3513–3517.
- (38) Eddingsaas, N. C.; Suslick, K. S. Evidence for a Plasma Core During Multibubble Sonoluminescence in Sulfuric Acid. *J. Am. Chem. Soc.* **2007**, *129*, 3838–3839.
- (39) Suslick, K. S.; Eddingsaas, N. C.; Flannigan, D. J.; Hopkins, S. D.; Xu, H. X. Extreme Conditions During Multibubble Cavitation: Sonoluminescence as a Spectroscopic Probe. *Ultrason. Sonochem.* **2011**, *18*, 842–846.
- (40) Xu, H. X.; Glumac, N. G.; Suslick, K. S. Temperature Inhomogeneity During Multibubble Sonoluminescence. *Angew. Chem., Int. Ed.* **2010**, *49*, 1079–1082.
- (41) Lehrer, T. A. Introduction to “We Will All Go Together When We Go”. In *An Evening Wasted with Tom Lehrer*; Reprise Records: Burbank, 1959.
- (42) Flannigan, D. J.; Suslick, K. S. Plasma Formation and Temperature Measurement During Single-Bubble Cavitation. *Nature* **2005**, *434*, 52–55.
- (43) Thiemann, A.; Holsteyns, F.; Cairós, C.; Mettin, R. Sonoluminescence and Dynamics of Cavitation Bubble Populations in Sulfuric Acid. *Ultrason. Sonochem.* **2017**, *34*, 663–676.

- (44) Flannigan, D. J.; Suslick, K. S. Emission from Electronically Excited Metal Atoms During Single-Bubble Sonoluminescence. *Phys. Rev. Lett.* **2007**, *99*, 134301.
- (45) Lohse, D.; Brenner, M. P.; Dupont, T. F.; Hilgenfeldt, S.; Johnston, B. Sonoluminescing Air Bubbles Rectify Argon. *Phys. Rev. Lett.* **1997**, *78*, 1359–1362.
- (46) Hilgenfeldt, S.; Lohse, D.; Brenner, M. P. Phase Diagrams for Sonoluminescing Bubbles. *Phys. Fluids* **1996**, *8*, 2808–2826.
- (47) Didenko, Y. T.; Suslick, K. S. The Energy Efficiency of Formation of Photons, Radicals and Ions During Single-Bubble Cavitation. *Nature* **2002**, *418*, 394–397.
- (48) Storey, B. D.; Szeri, A. J. Water Vapour, Sonoluminescence and Sonochemistry. *Proc. R. Soc. London, Ser. A* **2000**, *456*, 1685–1709.
- (49) Hiller, R. A.; Putterman, S. J.; Weninger, K. R. Time-Resolved Spectra of Sonoluminescing Bubbles. *Phys. Rev. Lett.* **1998**, *80*, 1090–1093.
- (50) Gompf, B.; Günther, R.; Nick, G.; Pecha, R.; Eisenmenger, W. Resolving Sonoluminescence Pulse Width with Time-Correlated Single Photon Counting. *Phys. Rev. Lett.* **1997**, *79*, 1405–1408.
- (51) Moss, W. C.; Clarke, D. B.; Young, D. A. Calculated Pulse Widths and Spectra of a Single Sonoluminescing Bubble. *Science* **1997**, *276*, 1398–1401.
- (52) Moss, W. C.; Clarke, D. B.; White, J. W.; Young, D. A. Hydrodynamic Simulations of Bubble Collapse and Picosecond Sonoluminescence. *Phys. Fluids* **1994**, *6*, 2979–2985.
- (53) Hammer, D.; Frommhold, L. Sonoluminescence: How Bubbles Glow. *J. Mod. Opt.* **2001**, *48*, 239–277.
- (54) Vazquez, G.; Camara, C.; Putterman, S. J.; Weninger, K. Blackbody Spectra for Sonoluminescing Hydrogen Bubbles. *Phys. Rev. Lett.* **2002**, *88*, 197402.
- (55) Didenko, Y. T.; McNamara, W. B., III; Suslick, K. S. Molecular Emission from Single-Bubble Sonoluminescence. *Nature* **2000**, *407*, 877–879.
- (56) Luque, J.; Crosley, D. R. *Lifbase, Database and Spectral Simulation for Diatomic Molecules* (V. 2.0.55); SRI International, 1999.
- (57) Didenko, Y. T.; McNamara, W. B., III; Suslick, K. S. Temperature of Multibubble Sonoluminescence in Water. *J. Phys. Chem. A* **1999**, *103*, 10783–10788.
- (58) Radziuk, D.; Mohwald, H.; Suslick, K. Single Bubble Perturbation in Cavitation Proximity of Solid Glass: Hot Spot Versus Distance. *Phys. Chem. Chem. Phys.* **2014**, *16*, 3534–3541.
- (59) McNamara, W. B., III; Didenko, Y. T.; Suslick, K. S. Pressure During Sonoluminescence. *J. Phys. Chem. B* **2003**, *107*, 7303–7306.
- (60) Flannigan, D. J.; Hopkins, S. D.; Camara, C. G.; Putterman, S. J.; Suslick, K. S. Measurement of Pressure and Density inside a Single Sonoluminescing Bubble. *Phys. Rev. Lett.* **2006**, *96*, 204301.
- (61) Flannigan, D. J.; Suslick, K. S. Inertially Confined Plasma in an Imploding Bubble. *Nat. Phys.* **2010**, *6*, 598–601.
- (62) Barber, B. P.; Putterman, S. J. Observation of Synchronous Picosecond Sonoluminescence. *Nature* **1991**, *352*, 318–320.
- (63) Matula, T. J.; Roy, R. A.; Mourad, P. D. Optical Pulse Width Measurements of Sonoluminescence in Cavitation-Bubble Fields. *J. Acoust. Soc. Am.* **1997**, *101*, 1994–2002.
- (64) Hilgenfeldt, S.; Grossmann, S.; Lohse, D. A Simple Explanation of Light Emission in Sonoluminescence. *Nature* **1999**, *398*, 402–405.
- (65) Flannigan, D. J.; Suslick, K. S. Plasma Line Emission During Single-Bubble Cavitation. *Phys. Rev. Lett.* **2005**, *95*, 044301.
- (66) Flannigan, D. J.; Suslick, K. S. Plasma Quenching by Air During Single-Bubble Sonoluminescence. *J. Phys. Chem. A* **2006**, *110*, 9315–9318.
- (67) Bataller, A.; Kappus, B.; Camara, C.; Putterman, S. Collision Time Measurements in a Sonoluminescing Microplasma with a Large Plasma Parameter. *Phys. Rev. Lett.* **2014**, *113*, 024301.
- (68) Kappus, B.; Bataller, A.; Putterman, S. J. Energy Balance for a Sonoluminescence Bubble Yields a Measure of Ionization Potential Lowering. *Phys. Rev. Lett.* **2013**, *111*, 234301.
- (69) Khalid, S.; Kappus, B.; Weninger, K.; Putterman, S. Opacity and Transport Measurements Reveal That Dilute Plasma Models of Sonoluminescence Are Not Valid. *Phys. Rev. Lett.* **2012**, *108*, 104302.
- (70) Kappus, B.; Khalid, S.; Chakravarty, A.; Putterman, S. Phase Transition to an Opaque Plasma in a Sonoluminescing Bubble. *Phys. Rev. Lett.* **2011**, *106*, 234302.
- (71) Xu, H. X.; Zeiger, B. W.; Suslick, K. S. Sonochemical Synthesis of Nanomaterials. *Chem. Soc. Rev.* **2013**, *42*, 2555–2567.
- (72) Hinman, J. J.; Suslick, K. S. Nanostructured Materials Synthesis Using Ultrasound. *Top. Curr. Chem.* **2017**, *375*, 12.
- (73) Suslick, K. S.; Price, G. J. Applications of Ultrasound to Materials Chemistry. *Annu. Rev. Mater. Sci.* **1999**, *29*, 295–326.
- (74) Luche, J.-L. *Synthetic Organic Sonochemistry*; Plenum: New York, 1998.
- (75) Cravotto, G.; Gaudino, E. C.; Cintas, P. On the Mechanochemical Activation by Ultrasound. *Chem. Soc. Rev.* **2013**, *42*, 7521–7534.
- (76) *Sonochemistry and the Acoustic Bubble*; Grieser, F., Choi, P. K., Enomoto, N., Harada, H., Okitsu, K., Yasui, K., Eds.; Elsevier Science Bv: Amsterdam, 2015.
- (77) Colmenares, J. C., Chatel, G., Eds. *Sonochemistry: From Basic Principles to Innovative Applications*; Springer: Cham, Switzerland, 2016.